Supporting Information

Degradation of Ethylene Carbonate Electrolytes of Lithium Ion Batteries via Ring Opening Activated by $LiCoO_2$ Cathode Surfaces and Electrolyte Species

Jonathon L. Tebbe[†], Thomas F. Fuerst[†,‡], Charles B. Musgrave*[,†,‡]

[†]Department of Chemical and Biological Engineering, University of Colorado, Boulder, Colorado 80309-0596

[‡]Department of Chemistry and Biochemistry, University of Colorado, Boulder, Colorado 80309-0215

*Address Correspondence to: email: charles.musgrave@colorado.edu

KEYWORDS *$LiCoO_2$ Cathode, Capacity Fading, Cathode Electrolyte Interphase, Ethylene Carbonate Ring Opening, Battery Cycling*

Table of Contents

1.$LiCoO_2$ Surface Model

In order to examine reactions at the surface of cathode particles, we first developed a periodic slab model of the reacting $LiCoO_2$ surface. All atoms of the $LiCoO_2$ slab were allowed to relax during geometry optimizations except the bottom atomic layer of the slab, which was constrained to the calculated bulk atomic positions to allow sufficient relaxation of the $LiCoO_2$ surfaces. All supercells employ a 15 Å vacuum gap between the adsorbate surface and the backside of the periodic image of the slab to minimize spurious interactions.

The bare $(10\bar{1}4)$ $LiCoO_2$ surface involves under-coordinated bridging surface O atoms and Co atoms. The surface energy is reduced by passivating these high-energy Co dangling bonds with various possible terminations. We studied the fractional termination of the $(10\bar{1}4)$ surface with hydrogen, oxygen, and hydroxyl to predict a realistic surface with minimal dangling bonds and under-coordinated surface Co for modeling the subsequent surface reactions; the formation energies of the various surface terminations considered are reported in Table S1. Specifically, we modeled; a) hydrogen termination of the surface O atoms (O-H), b) bridging oxygen termination of the surface Co centers (Co-O-Co), and c) hydroxyl termination of the surface Co and Li atoms (Co-OH and Li-OH, respectively). We found that hydroxyl termination of at least half of the exposed Co atoms most effectively passivates the Co dangling bonds at the $LiCoO_2$ surface.

Table S1: Average Formation Energies for Various Terminations of the $(10\bar{1}4)$ $LiCoO_2$ Surface Relative to the Bare Surface and H_2O

Termination Type	Fractional Coverage	$\bar{E}_f$ (eV)
OH^{*a}	0.5	0.24
OH^{*a}	1.0	0.44
Co^{*}-O-Co^{*b}	0.5	1.18
$CoOH^{*c}$	$0.1\bar{6}$	-1.02
$CoOH^{*c}$	$0.\bar{3}$	-1.37
$CoOH^{*c}$	0.5	-1.43
$CoOH^{*c}$	1.0	-1.43
$LiOH^{*d}$	$0.1\bar{6}$	-0.22

[a] O-H represents H termination of surface O atoms.
[b] Co^{*}-O-Co^{*} represents O termination bridging two neighboring surface Co atoms.
[c] Co-OH represents OH termination of surface Co atoms.
[d] Li-OH represents OH termination of surface Li atoms.

2. Oligomerization of EC into the Bulk Electrolyte

In order to study the initial formation of the cathode-electrolyte interphase, we examined the oligomerization of ethylene carbonate (EC) tethered to the cathode surface that propagates by continued ring opening of EC into the electrolyte. We find that subsequent ring opening of the

solvating EC occurs in a similar manner to ring opening of the EC adsorbed to the cathode surface; a solvating EC electrolyte molecule facilitates the ring-opening reaction by donating electron density from its carbonyl O atom to the dissociating C atom. We predict that this ring opening reaction that oligomerizes ethylene carbonate occurs with a barrier of 0.84 eV and is endothermic by 0.80 eV. This reaction has an activation energy 0.20 eV lower and a reaction enthalpy 0.14 eV less endothermic that ring opening of the directly adsorbed EC, suggesting relatively facile reverse reaction. However, the CH_2 group that dissociates from the carbonate has a calculated H-C-H angle of 111.8° at the transition state, suggesting a greater sp^3 character than other ring opening reactions.

The increased donation of electron density from the reacting ethylene carbonate at the reactant depopulates the C-O bonding orbital, and consequently weakens the C-O bond. Weakening this bond lengthens the ethylene C and ether O bond distance in the EC from 1.44 Å to 1.50 Å and reduces the barrier to cleave this bond. Thus, the charge transfer from the solvating ethylene carbonate to the reacted ethylene carbonate adsorbed to the cathode surface during the initial ring opening causes greater polarization in solvating EC electrolyte molecules compared to EC adsorbed to the $LiCoO_2$ surface, generating a more electrophilic ethylene C and activating the solvating EC for ring opening and monomer addition. Additionally, the reactant state of this second EC ring opening is a relatively high energy state compared to the adsorbed ethylene carbonate, which allows for relatively greater donation of electron density from a solvating EC in the product state. Thus, we predict that a higher degree of oxidation of the solvating EC yields lower barriers to form EC oligomer films on the $LiCoO_2$ cathode surface. While the barrier to ring opening is lower, subsequent ring opening is endothermic by 0.80 eV, suggesting that addition of ring-opened ethylene monomers is quickly reversed by a nearly barrierless back reaction and thus further oligomerization into the electrolyte by this mechanism is unlikely to occur. Consequently, we expect only short organic chains to develop on the cathode surface as a result of EC ring opening reactions.

3. CO_2 Formation at the $LiCoO_2$ Surface

In addition to studying the formation of ethylene carbonate oligomers tethered to the cathode surface to form organic films, we also examined ring opening of EC at the cathode surface to form CO_2. As the reaction proceeds to the transition state, the ethylene C and ether O bond of adsorbed ethylene carbonate dissociates, increasing from 1.48 Å to 2.39 Å at the transition state (see SI Figure 1). We predict ring opening involves H^+ transfer and dissociation of a C-O ether bond. Reaction at the cathode surface differs slightly compared to CO_2 formation activated by PF_5, since the solvating ethylene carbonate does not directly interact with the transferring H^+, but instead is separated at distance of ~3 Å from the reacting adsorbed ethylene carbonate. This absence of stabilization of the transition state, coupled with the weaker Lewis acid-base interaction of adsorbed EC with the $LiCoO_2$ surface, results in a reaction barrier too high to be active at LIB operating temperatures.

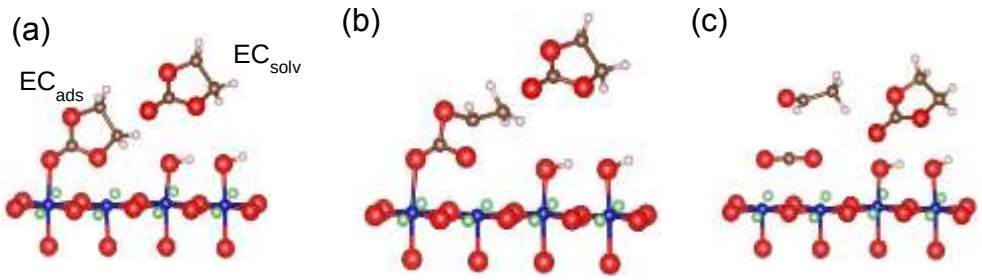

SI Figure 1. CO_2 formation via ring opening reaction of ethylene carbonate activated by interaction with the $LiCoO_2$ surface acting as a Lewis acid. EC ring opening to form CO_2 and acetaldehyde occurs with a barrier of 1.81 eV and a reaction energy of -0.50 eV. Shown above is: (a) EC adsorbed at two neighboring Co^* sites and (b) the transition state of EC ring opening, showing H^+ transfer, stabilized by charge donation from the solvating EC and (c) the CO_2 and acetaldehyde products. The atoms shown are Co (blue), O (red), Li (green), C (brown), H (white), F (light blue), and P (orange).

4. Coordinates of Molecular Structures

a. Ring Opening of a Single EC^+

Reactants

C	0.9	-0.040117	0.000067
O	2.0	0.03894	0.000179
O	0.0	1.113436	-0.000331
O	0.1	-1.106464	-0.00017
C	-1.3	-0.760296	0.000032
H	-1.8	-1.204458	-0.881191
H	-1.8	-1.205428	0.880595
C	-1.3	0.724992	0.000127
H	-1.8	1.246885	0.834928
H	-1.8	1.248234	-0.833113

Transition State

C	0.964964	0.130895	0.024512
O	2.104797	-0.260411	-0.151965
O	-0.009224	-0.97985	-0.070994
O	0.46408	1.234568	0.264636
C	-1.79808	0.53596	-0.268781
H	-2.73645	0.932659	0.115767
H	-1.400608	0.945963	-1.192561
C	-1.26847	-0.631347	0.256409
H	-2.080826	-1.043426	-0.542125
H	-1.649814	-1.002697	1.212655

Products

C	-2.3	-0.141492	-0.004545
O	-3.4	0.273113	0.038124
O	-1.2	-0.559296	-0.047568
C	1.8	-0.163366	0.021707
C	3.3	-0.111232	0.014336
O	1.1	0.797625	-0.027298
H	1.3	-1.160046	0.073332
H	3.6	0.915924	-0.011219
H	3.6	-0.65892	0.90895
H	3.6	-0.69195	-0.866116

b. Ring Opening Activated by PF_5

Reactants

P	3.838094	-0.15324	0.033859
F	4.151769	1.157807	0.886744
F	3.701281	0.746722	-1.288974
F	5.363543	-0.471507	-0.22808
F	3.780787	-1.018586	1.373101
F	3.333418	-1.427743	-0.803378
C	-3.46024	3.20878	-0.1131
O	-2.307928	3.256344	0.001313
O	2.054315	0.230426	0.401534
O	-4.612085	3.19006	-0.2351
C	-0.231965	0.462816	-0.084235
H	-0.644856	1.2046	-0.778316
H	-0.819311	-0.44995	-0.262846

C	1.149505	0.183581	-0.443867
H	-0.335623	0.78573	0.951725
H	1.400781	-0.084116	-1.478926
C	-3.763926	-0.680896	0.272847
O	-3.356865	0.415431	0.528519
O	-5.054316	-1.020987	0.233694
O	-2.976657	-1.725221	-0.014873
C	-3.783753	-2.838732	-0.4266
H	-3.7047	-2.93624	-1.512749
H	-3.404867	-3.741111	0.054103
C	-5.176127	-2.438101	0.037884
H	-5.459346	-2.893072	0.990909
H	-5.953327	-2.62058	-0.704786

Transition State

P	4.198898	0.163459	-0.036491
F	4.793234	-1.333538	-0.155959
F	4.060559	-0.024072	1.557505
F	5.686155	0.75568	0.150533
F	4.324769	0.327262	-1.638978
F	3.58036	1.649657	0.060513
C	1.361152	-0.29697	0.284127
O	2.476709	-0.583713	-0.329405
O	0.058582	-1.229994	-0.536103
O	0.765595	0.294981	1.145024
C	-1.782941	0.214962	-0.507805

H	-1.865402	0.961019	0.28615
H	-1.914812	0.220359	-1.592413
C	-1.19318	-1.078669	-0.000293
H	-2.492951	-1.099713	-0.012688
H	-1.153771	-1.073594	1.09349
C	-5.385537	-0.402998	0.022367
O	-4.480968	-1.282222	0.074167
O	-6.601162	-0.739641	0.247338
O	-5.151397	0.829535	-0.244923
C	-6.416779	1.559717	-0.166372
H	-6.318633	2.275718	0.64851
H	-6.549922	2.073673	-1.116637
C	-7.436878	0.449479	0.093348
H	-8.110531	0.260228	-0.741419
H	-7.997045	0.570837	1.01884

Products

P	3.838094	-0.15324	0.033859
F	4.151769	1.157807	0.886744
F	3.701281	0.746722	-1.288974
F	5.363543	-0.471507	-0.22808
F	3.780787	-1.018586	1.373101
F	3.333418	-1.427743	-0.803378
C	-3.46024	3.20878	-0.1131
O	-2.307928	3.256344	0.001313
O	2.054315	0.230426	0.401534

O	-4.612085	3.19006	-0.2351
C	-0.231965	0.462816	-0.084235
H	-0.644856	1.2046	-0.778316
H	-0.819311	-0.44995	-0.262846
C	1.149505	0.183581	-0.443867
H	-0.335623	0.78573	0.951725
H	1.400781	-0.084116	-1.478926
C	-3.763926	-0.680896	0.272847
O	-3.356865	0.415431	0.528519
O	-5.054316	-1.020987	0.233694
O	-2.976657	-1.725221	-0.014873
C	-3.783753	-2.838732	-0.4266
H	-3.7047	-2.93624	-1.512749
H	-3.404867	-3.741111	0.054103
C	-5.176127	-2.438101	0.037884
H	-5.459346	-2.893072	0.990909
H	-5.953327	-2.62058	-0.704786

c. Ring Opening without Activation by a Lewis Acid

Reactants

C	-5.241354	-0.07804	-0.018319
O	-4.120813	-0.489841	-0.109124
O	-6.335339	-0.828384	-0.178941
O	-5.557693	1.190902	0.257537
C	-6.976676	1.370053	0.135297
H	-7.324477	1.97562	0.972628

H	-7.177053	1.888483	-0.806539
C	-7.499984	-0.057778	0.153738
H	-8.270651	-0.24963	-0.593294
H	-7.851359	-0.37521	1.139462
C	0.812585	-0.435401	-0.084114
O	2.011222	-0.434874	-0.074371
O	0.063412	-1.53736	-0.14419
O	0.061799	0.666019	-0.035487
C	-1.330078	0.324337	-0.149153
H	-1.87273	0.814633	0.658647
H	-1.69678	0.691014	-1.110735
C	-1.329684	-1.197106	-0.044445
H	-1.864291	-1.688633	-0.856952
H	-1.704758	-1.563854	0.913934
C	6.875082	0.358581	0.072936
O	8.057815	0.547185	0.115539
O	6.291303	-0.81498	0.327972
O	5.975015	1.295327	-0.234935
C	4.655223	0.728627	-0.2681
H	4.002194	1.335027	0.359542
H	4.29327	0.752634	-1.29845
C	4.861874	-0.686565	0.26312
H	4.475831	-1.458734	-0.40222
H	4.455106	-0.833542	1.266233

Transition State

C	0.853594	-1.479417	-0.08151
O	1.625134	-1.783364	-0.9736
O	-0.499599	-2.027909	-0.326344
O	0.962746	-0.827453	0.962361
C	-1.430492	-0.595692	1.291987
H	-1.974752	-0.466318	2.22624
H	-1.131564	0.289415	0.738196
C	-1.356499	-1.844257	0.696564
H	-2.434308	-1.435406	0.324332
H	-1.616622	-2.72863	1.286437
C	-4.507341	-0.026564	-0.338165
O	-4.059539	-1.113308	-0.60025
O	-5.551455	0.521492	-0.94375
O	-4.000436	0.770611	0.603731
C	-4.661651	2.048825	0.555435
H	-4.891516	2.35722	1.575247
H	-3.980287	2.766675	0.092266
C	-5.894195	1.756119	-0.287369
H	-6.089743	2.508903	-1.050872
H	-6.794414	1.584135	0.307727
C	5.46303	1.22599	0.052753
O	6.339709	1.997352	0.32564
O	5.22623	0.091605	0.715733
O	4.600058	1.393906	-0.952263
C	3.607978	0.350586	-0.927448

H	2.660374	0.779294	-0.591183
H	3.496777	-0.045812	-1.936027
C	4.18046	-0.652074	0.062168
H	4.630884	-1.524811	-0.418017
H	3.453079	-0.969206	0.809096

Products

C	7.484805	-0.602288	0.171484
O	8.645805	-0.861337	0.305599
O	6.535741	-1.505759	-0.094405
O	6.971086	0.628109	0.26883
C	5.576377	0.606449	-0.063303
H	5.031688	1.1636 0.699844	
H	5.445668	1.088689	-1.03592
C	5.244078	-0.8814	-0.081946
H	4.699234	-1.193927	-0.97343
H	4.706245	-1.212427	0.81069
C	1.670447	1.420262	-0.091463
O	2.411848	0.576312	-0.377973
O	0.970939	2.296782	0.200007
C	-1.552791	0.353566	-0.038188
C	-2.900176	-0.256751	-0.172541
O	-0.51657	-0.194285	-0.340778
H	-1.530147	1.388691	0.370092
H	-2.83993	-1.261605	-0.597563
H	-3.380848	-0.289049	0.814306

H	-3.531898	0.386531	-0.798104
C	-6.309663	0.541231	-0.048843
O	-5.939487	1.66904	-0.202286
O	-6.929958	0.0894 1.046276	
O	-6.145653	-0.435098	-0.950318
C	-6.550257	-1.688168	-0.378633
H	-7.120658	-2.243959	-1.123159
H	-5.650872	-2.248994	-0.106658
C	-7.370461	-1.259226	0.827333
H	-7.166448	-1.84273	1.725452
H	-8.446209	-1.242186	0.631442